Sensors & Actuators: B. Chemical 348 (2021) 130717

Contents lists available at ScienceDirect

Sensors and Actuators: B. Chemical

journal homepage: www.elsevier.com/locate/snb

Competitive electrochemiluminescence aptasensor based on the Ru(II) derivative utilizing intramolecular ECL emission for E_2 detection

Qinqin Zhao [a], Jingwei Xue [a], Xiang Ren [a], Dawei Fan [a], Xuan Kuang [a], Yuyang Li [a,*], Qin Wei [a,*], Huangxian Ju [a,b]

[a] Collaborative Innovation Center for Green Chemical Manufacturing and Accurate Detection, Key Laboratory of Interfacial Reaction & Sensing Analysis in Universities of Shandong, School of Chemistry and Chemical Engineering, University of Jinan, Jinan 250022, PR China
[b] State Key Laboratory of Analytical Chemistry for Life Science, School of Chemistry and Chemical Engineering, Nanjing University, Nanjing 210023, PR China

ARTICLE INFO

Keywords:
Intramolecular electrochemiluminescence
Competitive
Aptasensor
$Ru(dcbpy)_3^{2+}$
Carbohydrazide

ABSTRACT

One competitive aptasensor based on novel intramolecular ECL emission system was investigated for ultrasensitive detection of E_2. It should be noted that the Ru(II) derivative for the mechanism of intramolecular ECL could improve electron transfer efficiency and reduce energy consumption. The Ru(II) derivatives were prepared by optimizing distribution ratio of $Ru(dcbpy)_3^{2+}$ and carbohydrazide for acquiring the ECL signal maximum. Stimulated by In^{3+}/In^{+} redox reversible electron pair in the $InVO_4/\beta$-$AgVO_3$ heterostructures, the $InVO_4/\beta$-$AgVO_3$ heterostructures were designed as co-reaction accelerator to expedite ECL emission reaction between $CON_4H_6^{\bullet}$ and $Ru(dcbpy)_3^{3+}$. Taking advantage of associative competition between cDNA and E_2 with aptamer, the ECL signal realized further amplification. The specific binding of the aptamer to E_2, was stronger than that to the cDNA by hybridization. A mass of Ru(II) derivatives could adsorb and embed into the hybridized double-stranded DNA to immobilize on the electrode surface and generate satisfactory ECL signal. The specific binding of the aptamer to E_2 decreased the cDNA content on electrode surface, which contributed to lessen the adsorption amount of $Ru(dcbpy)_3^{2+}$ and distinctly affected the ECL signal. Under optimal conditions, the proposed biosensor provided an admirable linearity to the level of E_2 between 0.001 nmol/L and 100 nmol/L with a low detection limit of 0.27 pmol/L. The proposed aptasensor not only stimulates more interest in the mechanism of intramolecular ECL but also has towardly development potential for constructing competitive strategies.

1. Introduction

Electrochemiluminescence, which could realize trace detection relying on light-emission process analysis, has been significant attention in immunoassay field [1–4]. A progressive ECL mode mainly depends on the prominent ECL performance of practical luminous mechanism [5,6]. The intermolecular ECL emission of emitter and co-reactant is frequently utilized in traditional research [7,8]. It is known that tris(4,4′-dicarboxylicacid-2,2′-bipyridyl) ruthenium(II) dichloride [$Ru(dcbpy)_3^{2+}$] can generate stable ECL signal with tripropylamine (TPrA) as the co-reactant utilizing the intermolecular ECL emission mechanism [9,10]. However, the increased reaction distance, depressed electron transfer rate and enhancive energy consumption limit its application [11–13].

To optimize this problem, this mode involved the Ru(II) derivative for the mechanism of intramolecular ECL emission, which could be obtained through an amide reaction between $Ru(dcbpy)_3^{2+}$ and carbohydrazide [14]. The intramolecular ECL reaction in system could improve reaction efficiency and suppress interference to realize ECL signal amplification [15]. Moreover, the optimal ratio of the Ru(II) derivative was investigated to present the satisfactory performance by designing different ratios of $Ru(dcbpy)_3^{2+}$ and carbohydrazide. Simultaneously, co-reaction accelerators play a key role in catalyzing co-reactants to form free radicals and promoting ECL emission. The co-reaction accelerators are actually special nanomaterials, which contain particles with different valence states and participate in redox reactions. Inspired by the fast and reversible conversion of redox couple In^{3+}/In^{+} in $InVO_4/\beta$-$AgVO_3$ heterostructures [16–19], $InVO_4/\beta$-$AgVO_3$ heterostructures were seen to be an appropriate co-reaction accelerator choice for fabrication of the ECL biosensor. The indispensable effect of $InVO_4/\beta$-$AgVO_3$ heterostructures in improving the ECL efficiency was verified by practicing in the intramolecular ECL mechanism of the Ru(II)

* Corresponding authors.
E-mail addresses: chm_liyy@ujn.edu.cn (Y. Li), sdjndxwq@163.com (Q. Wei).

https://doi.org/10.1016/j.snb.2021.130717
Received 5 July 2021; Received in revised form 16 August 2021; Accepted 4 September 2021
Available online 8 September 2021

derivative. Compared with blank samples, $InVO_4$/β-$AgVO_3$ heterostructures were be proved to expedite ECL emission reaction between $CON_4H_6^{\bullet}$ and $Ru(dcbpy)_3^{3+}$ and improve ECL efficiency.

A biosensor plays an important role in providing specific quantitative analytical information through detecting the binding event between a biorecognition element and target analyte [20,21]. Aptamer, as a biorecognition element, has emerged noteworthy advantages compared to antibody, such as higher specificity, greater design flexibility, more stable and available. More recently, the study with respect to the aptasensor has received ascending attention [9,22–25]. Thus, competitive aptasensor was introduced to further realize the ECL signal amplification in this work. 17β-estradiol (E_2), an effective biomarker for clinical diagnosis of breast cancer, and the cDNA can simultaneously interact with the aptamer to trigger binding competition. The cDNA can hybridize with the aptamer to form double-stranded DNA structure, and Ru (II) derivative can be involved into hybridized double-stranded DNA by means of adsorption and embedding to generate distinct ECL signal. However, as the hybridization power is weaker than the specific binding power of the aptamer to E_2, the amount of double-stranded DNA formation is regulated by the amount of E_2 modification. The specific

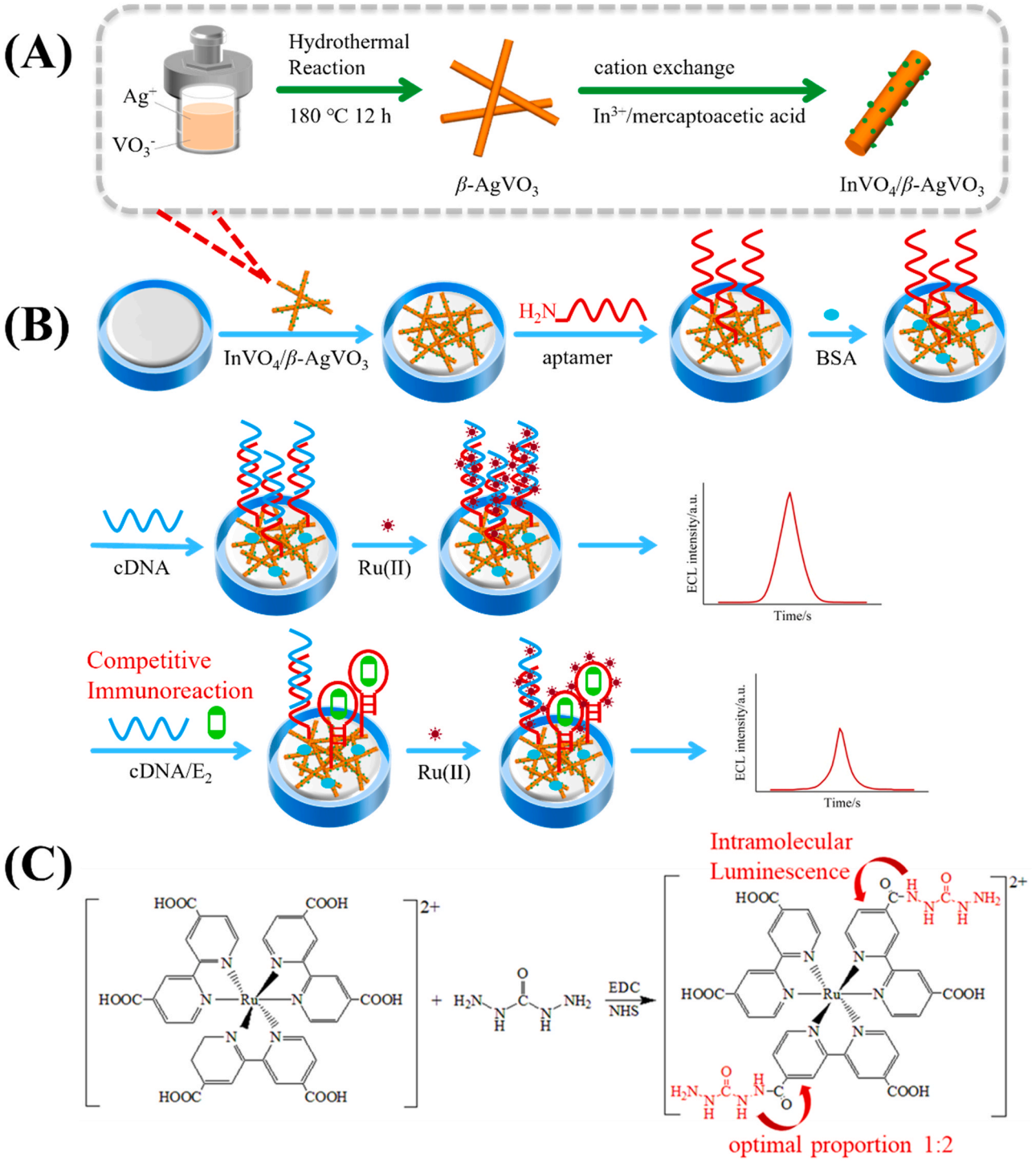

Scheme 1. Preparation process of $InVO_4$/β-$AgVO_3$ heterostructures (A), Fabrication process of the proposed competitive aptasensor (B), and synthesis route of the optimum Ru(II) derivative (C).

binding between aptamer and E_2 could be availably transduced into ECL signal amplification, thus various concentrations of E_2 could be accurately quantified.

Using cDNA as a detection probe, a super-sensitive competitive ECL aptasensor was presented to quantify detection of 17β-estradiol (E_2) in human serum (Scheme 1). Intramolecular ECL emission mechanism of the Ru(II) derivative clearly enhanced ECL intensity of the aptasensor which depended on a shorter electron transport distance and more efficient transmission speed. Above all, the optimal distribution ratio and ECL mechanism of the Ru(II) derivative were also discussed for achieving the advantageous performance of the aptasensor. With the help of catalytic activity of $InVO_4$/β-$AgVO_3$ heterostructures as co-reaction accelerator, the ECL emission efficiency of the Ru(II) derivative was improved. In addition, the competition between cDNA and E_2 could determine the amount of adsorption of the Ru(II) derivative to further improve the sensitivity of the aptasensor. This design provides a feasible idea for constructing ultrasensitive competitive aptasensors utilizing intramolecular ECL emission.

2. Experimental section

2.1. Preparation of Ru(II) derivative

This Ru(II) derivative was synthesized by the amide reaction of tris (4,4′-dicarboxylicacid-2,2′-bipyridyl) ruthenium(II) dichloride [Ru $(dcbpy)_3^{2+}$] with carbohydrazide (CON_4H_6) as shown in Scheme 1C. First, 400 μL of Ru$(dcbpy)_3^{2+}$ (1 mmol/L) was immersed into 100 μL PBS containing 40 mg EDC and 10 mg NHS to activate the carboxyl group of Ru$(dcbpy)_3^{2+}$. After adding 400 μL of carbohydrazide (25 mmol/L) to the above solution, the peptide bond was formed between the amino group of carbohydrazide and the carboxyl group of Ru $(dcbpy)_3^{2+}$ after an 8 h amide reaction. Finally, the novel Ru(II) derivative was collected by dialysis in secondary deionized water to separate small molecules. For comparison, the prepared Ru(II) derivatives were labeled as (x:y) Ru-CON_4H_6, where Ru, CON_4H_6, (x:y) represent Ru $(dcbpy)_3^{2+}$, carbohydrazide, and the molar ratio of Ru$(dcbpy)_3^{2+}$ and carbohydrazide in Ru(II) derivative, respectively. When the concentration of Ru$(dcbpy)_3^{2+}$ was immobilized, the actual carbohydrazide content of (2:1) Ru-CON_4H_6, (1:1) Ru-CON_4H_6, (1:2) Ru-CON_4H_6, and (1:3) Ru-CON_4H_6 samples were 0.25 mmol/L, 0.5 mmol/L, 1 mmol/L, 1.5 mmol/L. The synthesis of $InVO_4$/β-$AgVO_3$ heterostructures was shown in Supplementary Material.

2.2. Fabrication process of the competitive ECL aptasensor

The construction process of the competitive ECL aptasensor is shown in Scheme 1B. In the preparation process, the untreated glassy carbon electrode (GCE) was polished with Al_2O_3 polishing powder of different diameters on the suede until the surface of the electrode was mirrored, and then ultrasonically washed in ultrapure water and ethanol respectively for 3 min, and dried in N_2 atmosphere [26]. First, 6 μL $InVO_4$/-β-$AgVO_3$ heterostructures solution (9.5 mmol/L) was added on the pretreated GCE surface as the excellent conductive material of the system. After each layer of modification below, the modified electrode was rinsed with PBS (0.1 mmol/L, pH 7.4) to remove the unmodified substance [22,27,28]. In the following step , the amino-modified aptamer was immobilized on the surface of GCE/In-Ag heterostructures by oxygen-nitrogen bond and incubated at 37 °C for 1 h. After the GCE/In-Ag heterostructures/aptamer continuing to coat bovine serum albumin to block nonspecific active sites for capturing antigen, GCE/In-Ag heterostructures/aptamer/BSA was immersed in cDNA solution to capture cDNA by binding sites.

2.3. ECL measurement

After a series of different concentrations of E_2 covered in the GCE/In-Ag heterostructures/aptamer/BSA/cDNA surface, the aptamer specific combining with E_2 contributed sectional cDNA to detach from the electrode surface. Then, GCE/In-Ag heterostructures/aptamer/BSA/cDNA/E_2 was immersed in Ru(II) derivative solution to embed Ru(II) derivative molecules. Considering that the ECL signal gradually weakened as the E_2 concentration increased, an MPI-F ECL detector was selected for sensitive detection of E_2 through immersing the three-electrode system into 10 mL of PBS (0.1 mmol/L, pH 7.4). The ECL signal was acquired by the following three parameters: photosensitive multiplier voltage (800 V), cyclic voltammetry parameters (from 0 to 1.2 V), and scan rate (100 mV/s).

3. Results and discussion

3.1. Characterizations of $InVO_4$/β-$AgVO_3$ heterostructures

The band shaped $InVO_4$/β-$AgVO_3$ heterostructures synthesized via cation exchange and in situ growth process were utilized as the conductive substrate material in this system. X-ray diffraction (XRD), scanning electron microscope (SEM), transmission electron microscope (TEM) and high-resolution transmission electron microscopy (HRTEM) were used to investigate the morphology and fine-structure of the $InVO_4$/β-$AgVO_3$ heterostructures. The XRD pattern was displayed in Fig. 1A, and the diffraction peaks of 20.6°, 28.4°, 29.8°, 33.5°, 34.4°, 34.9°, 44.1° were identified as (301), (−211), (501), (−112), (−602), (112), (710) planes of monoclinic phase β-$AgVO_3$. Furthermore, the diffraction peaks on the (110), (111), (112), (130), (202), (042), (312) plane of orthorhombic phase $InVO_4$ showed up at 18.6°, 23.0°, 33.1°, 35.2°, 41.7°, 51.0°, 56.5°. As shown in Fig. S1, the band shaped $InVO_4$/β-$AgVO_3$ heterostructures morphology showed a matte texture on account of the rod-like β-$AgVO_3$ surface with abundant $InVO_4$ small particles, which indicated that the $InVO_4$/β-$AgVO_3$ heterostructures were successfully synthesized. It could be learnt from the SEM phenograms that the $InVO_4$/β-$AgVO_3$ heterostructures prepared by hydrothermal method were uniform, nanoribbon with a diameter of approximately 150 nm. Densely packed numerous nanoribbons increased the electroactive area and the reaction sites, which also accelerated electron transfer along the ordered array. The Fig. S1 likewise showed the elemental mapping images of $InVO_4$/β-$AgVO_3$ heterostructures and the distribution of Ag, In, V and O in $InVO_4$/β-$AgVO_3$ heterostructures could be obtained. Fig. 1B and C showed the TEM characterizations of $InVO_4$/β-$AgVO_3$ compound, which declared that the diameter of the $InVO_4$ nanoparticles was approximately 30 nm. It could be further confirmed from the Fig. 1B and C that $InVO_4$ nanoparticles were uniformly dispersed on the surface of β-$AgVO_3$ nanoribbons without agglomeration. From the HRTEM image of $InVO_4$/β-$AgVO_3$ heterostructures, the crystal planes and spacings could be seen clearly. Moreover, the electroactive surface area of $InVO_4$/β-$AgVO_3$ heterostructures was described in the Supplementary Material. Consequently, all these performances illustrated the $InVO_4$/β-$AgVO_3$ complex with admirable physicochemical properties to increase detection when used in facility.

3.2. Feasibility analysis of Ru(II) derivative of intramolecular ECL for ECL aptasensor

It is worth mentioning that Ru(II) derivative using the principle of intramolecular ECL significantly improved the signal for facilitating trace analysis and detection. Compared with the principle of intermolecular ECL, intramolecular ECL decreased the reaction distance, reduced the energy consumption, and avoided the uncertain interference caused by the co-reactant in the electrolyte. As shown in Fig. 2A, the ECL signal of Ru(II) derivative (curve d) was the highest. The Ru $(dcbpy)_3^{2+}$ had not co-reactant to accelerate electron transfer, therefore the signal of curve b was weaker. When CON_4H_6 was added to Ru $(dcbpy)_3^{2+}$ electrolyte (curve c), increasing reaction distance and interference generated signal intensity to rank only second to Ru(II)

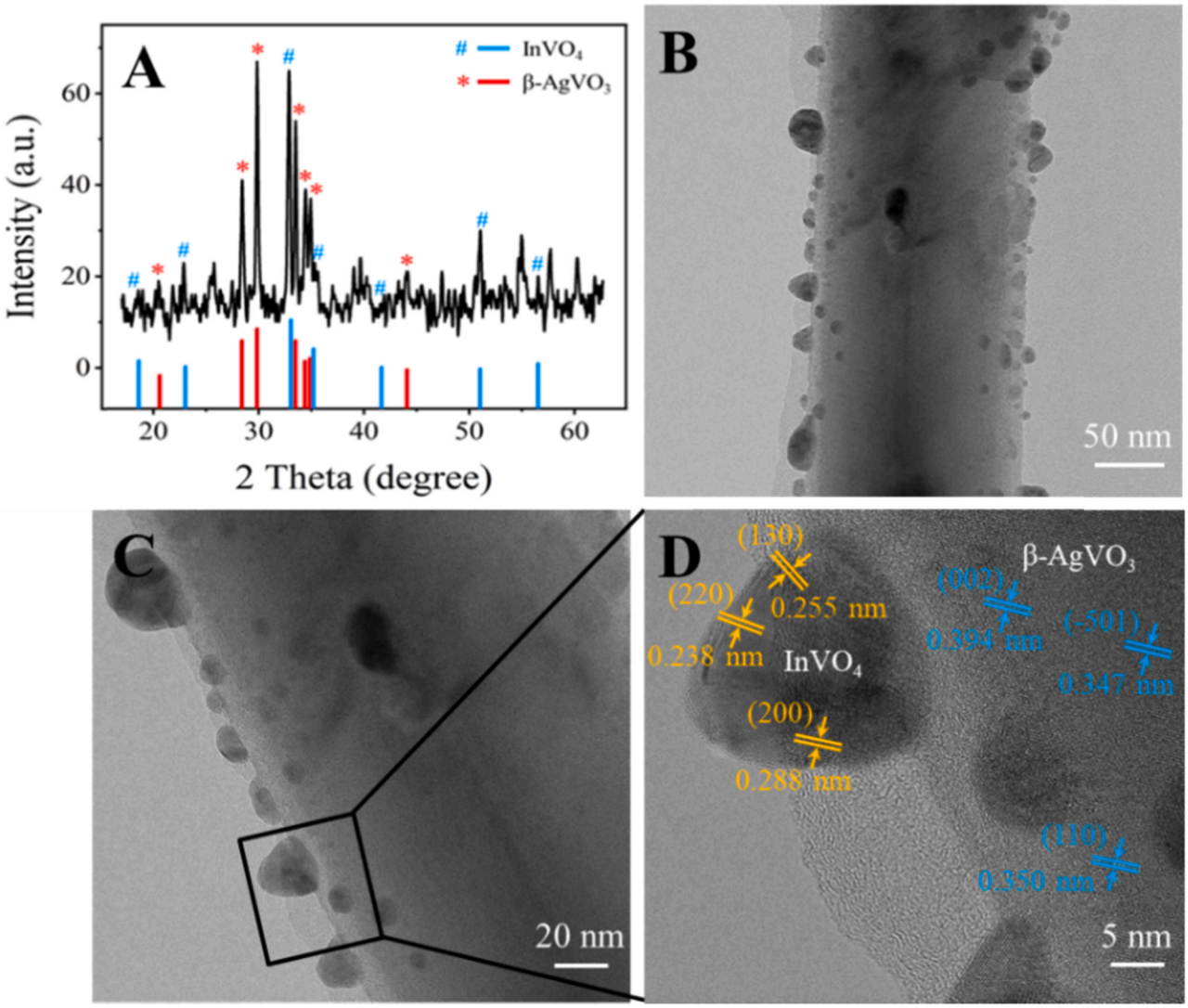

Fig. 1. XRD pattern (A), TEM images (B-C) and HRTEM image (D) of $InVO_4/\beta$-$AgVO_3$ heterostructures.

derivative. Hence, the intramolecular ECL mechanism has a wide range of application in trace analysis.

3.3. Optimal proportion of $Ru(dcbpy)_3^{2+}$ and CON_4H_6 for intramolecular ECL

In this intramolecular ECL system, the disparate molar ratios of Ru $(dcbpy)_3^{2+}$ and CON_4H_6 in Ru(II) derivative were researched as Fig. 2B shown. It was observed that when the molar ratio of $Ru(dcbpy)_3^{2+}$ and CON_4H_6 in Ru(II) derivative was (1:2), the ECL signal obtained the maximum. Since $Ru(dcbpy)_3^{2+}$ was quantitative, the ECL intensity showed an upward trend from (2:1) to (1:2) as the amount of CON_4H_6 increased to boost electron transfer and amplify the signal. Nevertheless, if there were too much CON_4H_6 in Ru(II) derivative, the ECL signal did not achieve the desired effect and the property of overall system was affected. Therefore, we optimized the molar ratio of $Ru(dcbpy)_3^{2+}$ and CON_4H_6 in Ru(II) derivative and obtained the optimal molar ratio of (1:2). The structural formulas of Ru(II) derivative in varying proportions were shown in Fig. 2C.

3.4. Discussion of competition mechanism between cDNA and E_2

To inquire the competition mechanism between cDNA and E_2 involved in the ECL system, electrode modified without E_2 was detected in PBS (pH 7.4). As shown in Fig. 3A, $Ru(dcbpy)_3^{2+}$, as a signal molecule, could be embedded in the molecular chain gap between aptamer and cDNA, which enhanced the ECL signal. When E_2 was not present, the maximum amount of $Ru(dcbpy)_3^{2+}$ was absorbed by the electrode surface to maximize the ECL intensity. However, the specific binding between E_2 and aptamer decreased cDNA content on the electrode surface, which contributed to lessen the adsorption amount of $Ru(dcbpy)_3^{2+}$ and obviously affected the ECL signal. The quantitative detection of E_2 was realized based on the changes of ECL signal before and after the presence of E_2.

3.5. Mechanism investigation of the intramolecular ECL of Ru(II) derivative

The intramolecular ECL appeared anodic response accompanying by the co-reactant CON_4H_6, when the cyclic voltage ranged from 0 to 1.2 V. The possible intramolecular ECL mechanism was indicated as follows. Under voltage excitation, the oxidation process of CON_4H_6 was slow (1). Therefore, by using $InVO_4/\beta$-$AgVO_3$ heterostructures as co-reaction accelerator, the yield of $CON_4H_6^{\bullet+}$ was greatly accelerated (2). After the deprotonation of $CON_4H_6^{\bullet+}$, the radical of CON_4H_6 ($CON_4H_6^{\bullet}$) was generated (3). The $CON_4H_6^{\bullet+}$ radical species oxidized $Ru(dcbpy)_3^{2+}$ to form $Ru(dcbpy)_3^{3+}$ which further reacted with the reductive substance ($CON_4H_6^{\bullet}$) to generate $Ru(dcbpy)_3^{2+*}$ (4) and (5). In this way, abundant

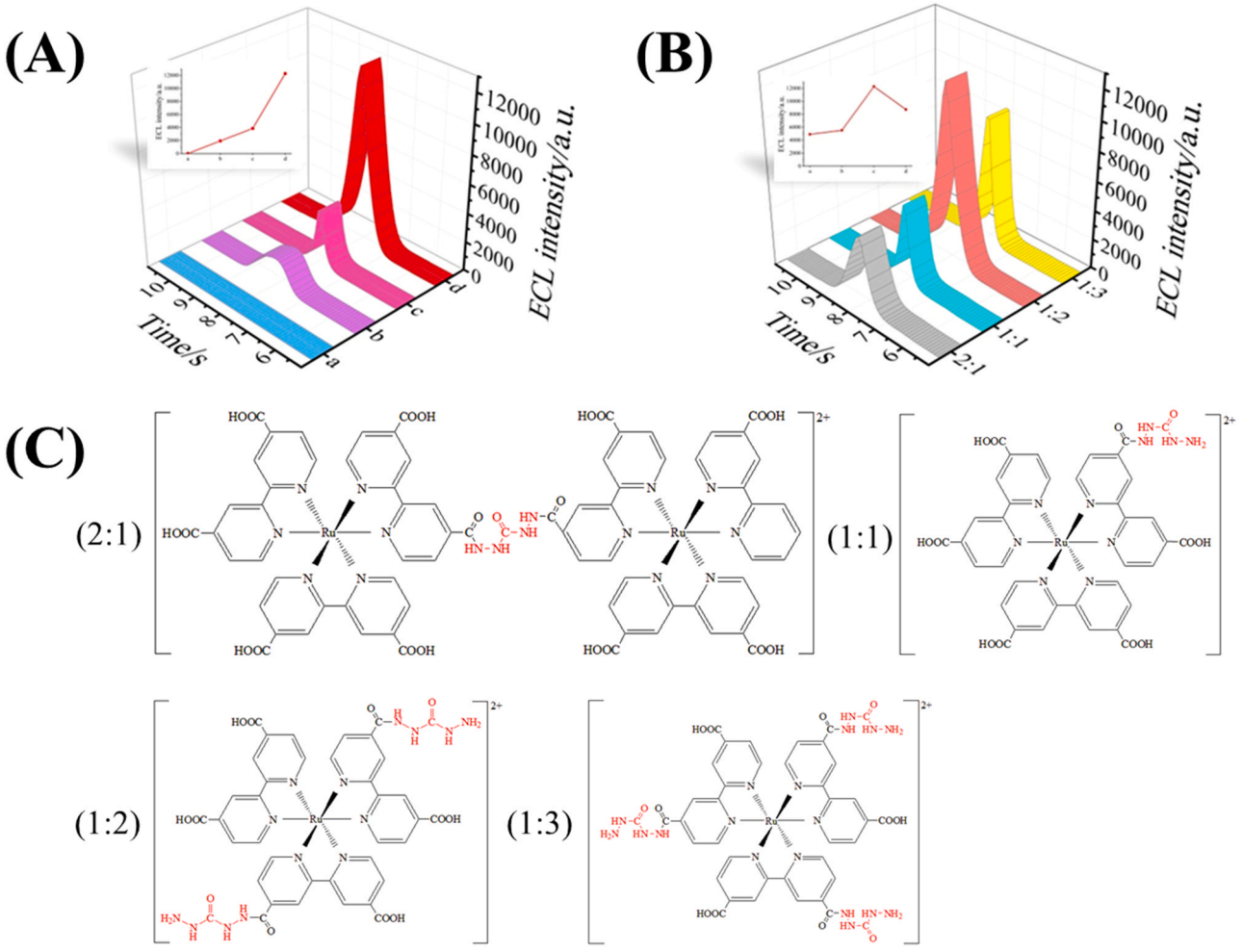

Fig. 2. ECL-time curves (A) of CON_4H_6 (a), $Ru(dcbpy)_3^{2+}$ (b), $Ru(dcbpy)_3^{2+}$ with CON_4H_6 in the electrolyte (c) and the prepared Ru(II) derivative (d). ECL-time curves (B) and structural formulas (C) of Ru(II) derivative in varying proportions.

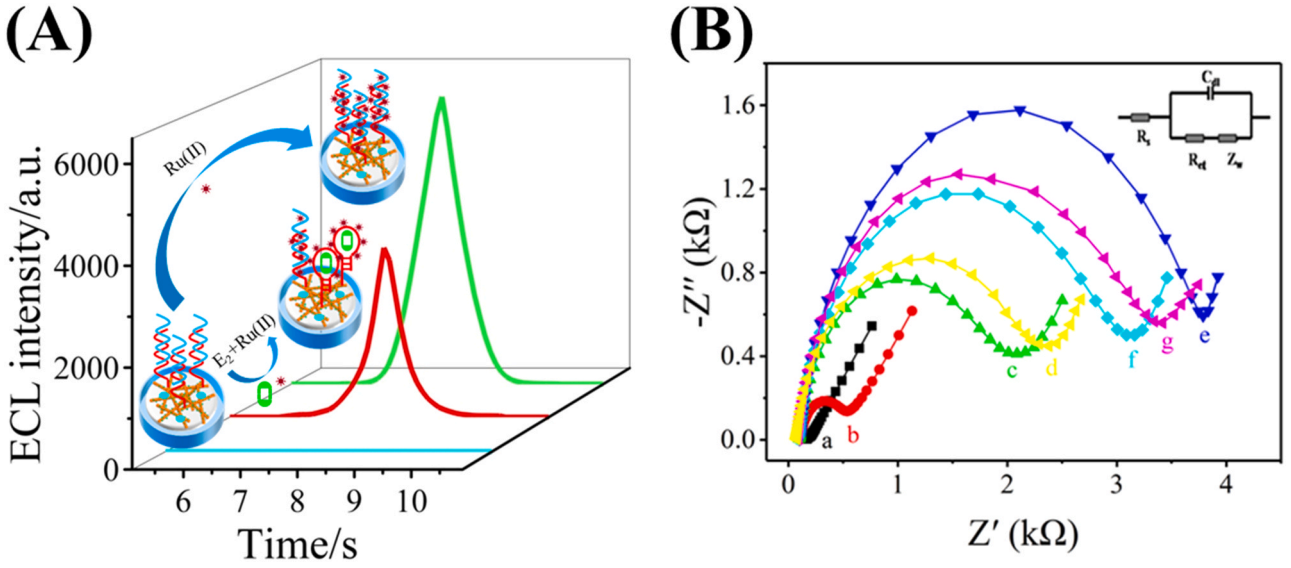

Fig. 3. ECL signal competition mechanism (A) and EIS analysis (B) of bare GCE (curve a), GCE/In-Ag heterostructures (curve b), GCE/In-Ag heterostructures/aptamer (curve c), GCE/In-Ag heterostructures/aptamer/BSA (curve d), GCE/In-Ag heterostructures/aptamer/BSA/cDNA (curve e), GCE/In-Ag heterostructures/aptamer/BSA/cDNA/E_2 (curve f), GCE/In-Ag heterostructures/aptamer/BSA/cDNA/E_2/Ru(II) derivative (curve g).

excited state $Ru(dcbpy)_3^{2+*}$ species reversed back to the steady state to obtain superior amplified signal (6).

$$CON_4H_6 - e \rightarrow 2CON_4H_6^{\bullet +} \text{ (less)} \quad (1)$$

$$InVO_4/\beta\text{-}AgVO_3\ (In^{III}) + 2CON_4H_6 \rightarrow 2CON_4H_6^{\bullet +}\ \text{(more)} + InVO_4/\beta\text{-}AgVO_3(In^{I}) \quad (2)$$

$$CON_4H_6^{\bullet +} - H^+ \rightarrow CON_4H_6^{\bullet} \quad (3)$$

$$CON_4H_6^{\bullet +} + Ru(dcbpy)_3^{2+} \rightarrow Ru(dcbpy)_3^{3+} + CON_4H_6 \quad (4)$$

$$CON_4H_6^{\bullet} + Ru(dcbpy)_3^{3+} \rightarrow Ru(dcbpy)_3^{2+*} + CON_4H_6 \quad (5)$$

$$Ru(dcbpy)_3^{2+*} \rightarrow Ru(dcbpy)_3^{2+} + hv \quad (6)$$

3.6. Characterization of the competitive ECL aptasensor

Electrochemical impedance spectroscopy (EIS) and cyclic voltammetry (CV) were used to characterize the layer by layer modification of the ECL aptasensor (electrolyte: 2.5 mmol/L $[Fe(CN)_6]^{4-/3-}$ and 0.1 mol/L KCl). As shown in Fig. 3B, the larger Nyquist circle radius represented by the modified electrode corresponds to the larger charge transfer resistance (Ret) [29]. GCE/In-Ag heterostructures (curve b) revealed a smaller Nyquist semicircle diameter on account of the acceleration of electron transmission by $InVO_4/\beta$-$AgVO_3$ heterostructures. Obviously, after the successive modification of aptamer, BSA, cDNA on the GCE surface, resistance value (curve c–e) enlarged sequentially, which could be ascribed to electrostatic repulsion between negatively charged phosphate skeleton and $[Fe(CN)_6]^{4-/3-}$. After immobilization of E_2, semicircle diameter decreased obviously (curve d), which was deemed that the presence of E_2 reduced the volume of cDNA on the electrode surface and lowered the electrostatic repulsion. After the final modification of $Ru(dcbpy)_3^{2+}$ (curve f), the resistance further increased. Therefore, the EIS spectrum confirmed the successful construction of the competitive ECL aptasensor. Simulation parameters of equivalent circuit components were shown in Table S1. The CV curves shown in Fig. S4, further indicated that the proposed ECL aptasensor was successful constructed.

3.7. Analytical ability of the competitive ECL aptasensor for E_2 detection

Under optimal experimental conditions, a series of concentration gradients of E_2 were incubated on the electrode surface to confirm the detection capability of the ECL aptasensor, as shown in Fig. 4A. There was a linear relationship between ECL response (I_{ECL}) and the logarithm of the concentration of E_2 (lg c), and the linear regression equation was $I = 1599.8 - 604.3 \lg c$ with a correlation index of 0.997 as shown in Fig. 4B. The competitive ECL aptasensor represented a wide detection range from 0.001 to 100 nmol/L with a detection limit of 0.27 pmol/L (S/N = 3), which was lower than other previous works listed in Table S2 [30–33].

3.8. Specificity, stability, and reproducibility of the aptasensor

For demonstrating the applicability of the aptasensor, specificity, stability and reproducibility of the aptasensor were measured. The specificity of the ECL aptasensor was investigated by measuring E_2 (2 nmol/L) with interfering substances (2 nmol/L) in human serum including α-fetoprotein (AFP), immunoglobulin G (IgG), prostate-

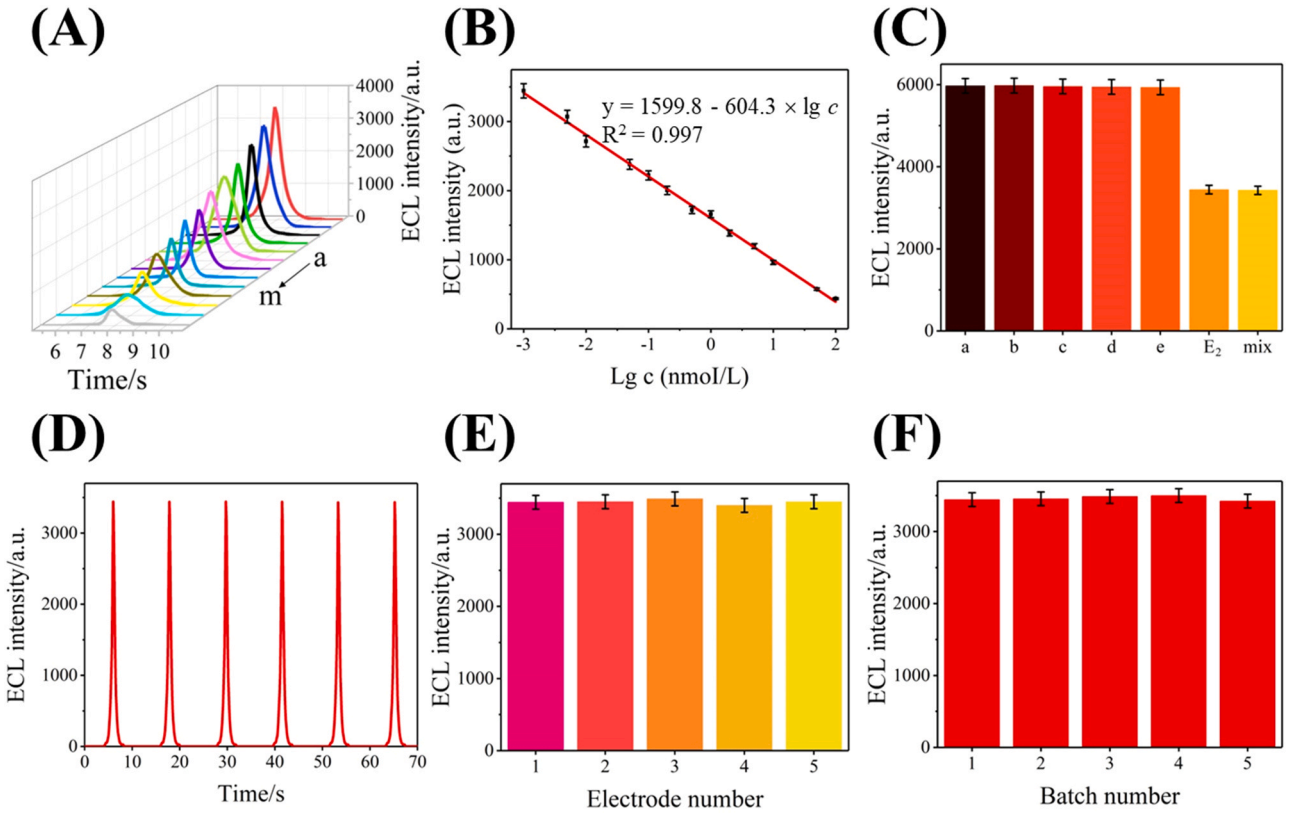

Fig. 4. ECL-time spectrum (A) and calibration curve (B) of the aptasensor incubated with various concentrations of E_2: 0.001 nmol/L (curve a), 0.005 nmol/L (curve b), 0.01 nmol/L (curve c), 0.05 nmol/L (curve d), 0.1 nmol/L (curve e), 0.2 nmol/L (curve f), 0.5 nmol/L (curve g), 1 nmol/L (curve h), 2 nmol/L (curve i), 5 nmol/L (curve j), 10 nmol/L (curve k), 50 nmol/L (curve l), 100 nmol/L (curve m). Specificity of the aptasensor (C) incubated without object (blank) and with various objects: AFP (a), IgG (b), PSA (c), CEA (d), CYFRA21-1 (e), E_2 and mixture. Stability of the aptasensor (D) for 6 cycles. Reproducibility of the aptasensor examined by inter-assay (E) and intra-assay (F) precision.

specific antigen (PSA), carcinoembryonic antigen (CEA) and cytokeratin 19 fragment 21-1 (CYFRA21-1) under the same conditions. As displayed in Fig. 4C, interfering substances had the signals equivalent to the blank sample, which did not play a role in the competition effect. It was evident that the signals of mixed samples (2 nmol/L of E_2 and 8 nmol/L of interferent) and E_2 were significantly lower, indicating the favourable specificity of the aptasensor. The aptasensor stability was studied by scanning the same electrode incubated with E_2 (2 nmol/L) for 6 cycles in succession. Fig. 4D showed that 6 peaks were comparable with an RSD of 3.83%, which emerged advantageous stability. What's more, five different ECL aptasensors incubated with E_2 (2 nmol/mL) in the same batch (Fig. 4E) and the same ECL aptasensor incubated with E_2 (2 nmol/mL) in five different batches (Fig. 4F) were detected for verifying reproducibility. It could be immediately seen from the diagram that the aptasensor had good reproducibility, with inter- and intra-assay relative standard deviations (RSD) equal to 1.46% and 3.31%.

3.9. Analytical application in human serum

In order to research the precision and application of this aptasensor, the standard addition method was utilized to detect different concentrations of E_2 in human serum. According to the linear curve (Fig. 4B), once the ECL signal recorded, the concentration of E_2 in human serum could be calculated. The recovery values were shown in Table 1 from 99.0% to 110% with RSD values from 0.511% to 1.17% (n = 11), which were the rate of the added concentration to the detected concentration. Hence, the proposed ECL aptasensor exhibited great prospect for detecting the concentration of E_2 in human serum.

4. Conclusion

Conclusively, a competitive electrochemiluminescence aptasensor based on Ru(II) derivative utilizing intramolecular ECL emission mechanism was presented. Intramolecular ECL reaction clearly improved electron transfer efficiency to enhance blank signal intensity of the signal-off aptasensor. In addition, it was obvious that the Ru(II) derivatives with a molar ratio of (1:2) had the satisfactory luminous performance through investigating the disparate molar ratios of Ru(dcbpy)$_3^{2+}$ and CON_4H_6 in Ru(II) derivatives. Therefore, the Ru(II) derivatives of (1:2) were selected as the signal probe in this aptasensor. At the same time, based on the fast and reversible conversion of redox couple In^{3+}/In^{+} in $InVO_4$/β-$AgVO_3$ heterostructures, $InVO_4$/β-$AgVO_3$ heterostructures were selected as the substrate and co-reaction accelerator to achieve signal amplification. What's more, the hybridization ability of cDNA and aptamer was weaker than the specific binding ability of aptamer to E_2. The binding competition between cDNA and E_2 changed the amount of embedding of the Ru(II) derivative and enlarged the change of ECL signal, which was advantageous for enhancing sensitivity of the aptasensor. The advanced immunosensor accomplished ultrasensitive E_2 detection in the range of 0.001 nmol/L and 100 nmol/L with a low detection limit of 0.27 pmol/L. We hope this ECL mode could inspire development of intramolecular ECL mechanism and provide a feasibility study for the competitive aptasensor to realize signal-amplification in bioanalysis.

CRediT authorship contribution statement

Qinqin Zhao: Conceived and designed the experiments, Performed the experiments, Analyzed the data and Wrote the first draft of the manuscript. **Jingwei Xue:** Conceived and designed the experiments. **Xiang Ren:** Contributed substantially to revisions. **Dawei Fan:** Contributed substantially to revisions. **Xuan Kuang:** Contributed substantially to revisions. **Yuyang Li:** Contributed substantially to revisions. **Qin Wei:** Contributed substantially to revisions. **Huangxian Ju:** Contributed substantially to revisions. All the authors discussed the results and commented on the manuscript.

Table 1
Recovery data of different concentrations of E_2 by the standard addition method.

Initial concentration (nmol/L)	Added concentration (nmol/L)	Average concentration (nmol/L, n = 11)	RSD (%, n = 11)	Recovery (%)
2.20	0.100	2.31	0.588	110
	3.00	5.19	1.17	99.7
	10.0	12.1	0.511	99.0

Declaration of Competing Interest

The authors declare that they have no known competing financial interests or personal relationships that could have appeared to influence the work reported in this paper.

Acknowledgements

This study was supported by the National Key Scientific Instrument and Equipment Development Project of China (No. 21627809), National Natural Science Foundation of China (Nos. 21607055, 21775053 and 21777056), the Natural Science Foundation of Shandong Province (No. 2019GSF111023), Jinan Scientific Research Leader Workshop Project (2018GXRC024), the Innovation Team Project of Colleges and Universities in Jinan (No. 2019GXRC027).

Appendix A. Supporting information

Supplementary data associated with this article can be found in the online version at doi:10.1016/j.snb.2021.130717.

References

[1] J. Wu, A. Wang, P. Liu, Y. Hou, L. Song, R. Yuan, Y. Fu, Sulfur-functionalized zirconium(IV)-based metal-organic frameworks relieves aggregation-caused quenching effect in efficient electrochemiluminescence sensor, Sens. Actuators B: Chem. 321 (2020), 128531.
[2] W. Liang, Y. Zhuo, C. Xiong, Y. Zheng, Y. Chai, R. Yuan, A sensitive immunosensor via in situ enzymatically generating efficient quencher for electrochemiluminescence of iridium complexes doped SiO2 nanoparticles, Biosens. Bioelectron. 94 (2017) 568–574.
[3] J. Liu, R. Zhao, X. Wang, X. Gao, G. Zou, Mechanistic investigations into synergistically enhanced radiative-charge-transfer in Au–Ag bimetallic nanoclusters, Chem. Commun. 56 (2020) 5665–5668.
[4] X. Long, F. Zhang, Y. He, S. Hou, B. Zhang, G. Zou, Promising anodic electrochemiluminescence of nontoxic core/shell CuInS2/ZnS nanocrystals in aqueous medium and its biosensing potential, Anal. Chem. 90 (2018) 3563–3569.
[5] L. Yang, Y. Jia, D. Wu, Y. Zhang, H. Ju, Y. Du, H. Ma, Q. Wei, Synthesis and application of CeO_2/SnS_2 heterostructures as a highly efficient coreaction accelerator in the luminol–dissolved O_2 system for ultrasensitive biomarkers immunoassay, Anal. Chem. 91 (2019) 14066–14073.
[6] X. Wang, Q. Zhang, Q. Kang, G. Zou, D. Shen, A high sensitive single luminophore ratiometric electrochemiluminescence immunosensor in combined with anodic stripping voltammetry, Electrochim. Acta 336 (2020), 135725.
[7] Z. Li, S. Wu, B. Zhang, L. Fu, G. Zou, Promising mercaptobenzoic acid-bridged charge transfer for electrochemiluminescence from $CuInS_2$@ZnS nanocrystals via internal Cu^{+}/Cu_2^{+} couple cycling, J. Phys. Chem. Lett. 10 (2019) 5408–5413.
[8] J. Shu, Z. Han, T. Zheng, D. Du, G. Zou, H. Cui, Potential-resolved multicolor electrochemiluminescence of N-(4-Aminobutyl)-N-ethylisoluminol/tetra(4-carboxyphenyl)porphyrin/TiO_2 nanoluminophores, Anal. Chem. 89 (2017) 12636–12640.
[9] Y. Zhang, J. Wang, S. Chen, R. Yuan, A novel magnetic beads-assisted highly-ordered enzyme-free localized DNA cascade reaction for the fluorescence detection of Pb_2^{+}, Sens. Actuators B: Chem. 342 (2021), 130040.
[10] Y. Huang, X. Zhu, C. Jin, W. Li, Y. Zhou, R. Yuan, Double-site DNA walker based ternary electrochemiluminescent biosensor, Talanta 219 (2020), 121274.
[11] H. Wang, Y. Chai, H. Li, R. Yuan, Sensitive electrochemiluminescent immunosensor for diabetic nephropathy analysis based on tris(bipyridine) ruthenium(II) derivative with binary intramolecular self-catalyzed property, Biosens. Bioelectron. 100 (2018) 35–40.
[12] X. Jiang, H. Wang, Y. Chai, W. Shi, R. Yuan, High-efficiency CNNS@NH_2-MIL(Fe) electrochemiluminescence emitters coupled with Ti3C2 nanosheets as a matrix for a highly sensitive cardiac Troponin I assay, Anal. Chem. 92 (2020) 8992–9000.
[13] S. Liu, Y. Jia, H. Dong, X. Yu, D.-P. Zhang, X. Ren, Y. Li, Q. Wei, Intramolecular photoelectrochemical system using tyrosine-modified antibody-targeted peptide as electron donor for detection of biomarkers, Anal. Chem. 92 (2020) 10935–10939.

[14] L. Fu, B. Zhang, K. Fu, X. Gao, G. Zou, Electrochemically lighting up luminophores at similar low triggering potentials with mechanistic insights, Anal. Chem. 92 (2020) 6144–6149.
[15] J. Luo, D. Liang, X. Li, S. Liu, L. Deng, F. Ma, Z. Wang, M. Yang, X. Chen, Photoelectrochemical detection of human epidermal growth factor receptor 2 (HER2) based on Co_3O_4-ascorbic acid oxidase as multiple signal amplifier, Mikrochim. Acta 188 (2021) 166.
[16] Y. Yang, Q. Yan, Q. Liu, Y. Li, H. Liu, P. Wang, L. Chen, D. Zhang, Y. Li, Y. Dong, An ultrasensitive sandwich-type electrochemical immunosensor based on the signal amplification strategy of echinoidea-shaped Au@Ag-Cu_2O nanoparticles for prostate specific antigen detection, Biosens. Bioelectron. 99 (2018) 450–457.
[17] Y. Yang, Q. Liu, Y. Liu, J. Cui, H. Liu, P. Wang, Y. Li, L. Chen, Z. Zhao, Y. Dong, A novel label-free electrochemical immunosensor based on functionalized nitrogen-doped graphene quantum dots for carcinoembryonic antigen detection, Biosens. Bioelectron. 90 (2017) 31–38.
[18] X. Li, J. Luo, L. Deng, F. Ma, M. Yang, In situ incorporation of fluorophores in zeolitic imidazolate framework-8 (ZIF-8) for ratio-dependent detecting a biomarker of anthrax spores, Anal. Chem. 92 (2020) 7114–7122.
[19] T. Gan, Z. Wang, Z. Shi, D. Zheng, J. Sun, Y. Liu, Graphene oxide reinforced core–shell structured Ag@Cu_2O with tunable hierarchical morphologies and their morphology–dependent electrocatalytic properties for bio-sensing applications, Biosens. Bioelectron. 112 (2018) 23–30.
[20] H.-H. Wang, M.-J. Li, Y.-P. Tu, H.-J. Wang, Y.-Q. Chai, Z.-H. Li, R. Yuan, Fullerenol as a photoelectrochemical nanoprobe for discrimination and ultrasensitive detection of amplification-free single-stranded DNA, Biosens. Bioelectron. 173 (2021), 112802.
[21] Z. Wu, S. Liu, Y. Li, F. Tang, Z. Zhao, Q. Liu, Y. Li, Q. Wei, Electrochemiluminescence resonance energy transfer system fabricated by quantum state complexes for cardiac troponin I detection, Sens. Actuators B: Chem. 336 (2021), 129733.
[22] Y. Guo, F. Yang, Y. Yao, J. Li, S. Cheng, H. Dong, H. Zhang, Y. Xiang, X. Sun, Novel Au-tetrahedral aptamer nanostructure for the electrochemiluminescence detection of acetamiprid, J. Hazard. Mater. 401 (2021), 123794.
[23] L. Liu, Y. Zhang, R. Yuan, H. Wang, Ultrasensitive electrochemiluminescence biosensor using sulfur quantum dots as an emitter and an efficient DNA walking machine with triple-stranded DNA as a signal amplifier, Anal. Chem. 92 (2020) 15112–15119.
[24] C. Li, Z. Chen, Y. Zhang, J. He, R. Yuan, W. Xu, Guanine-lighting-up fluorescence biosensing of silver nanoclusters populated in functional DNA constructs by a pH-triggered switch, Anal. Chem. 92 (2020) 13369–13377.
[25] Z. Lv, Q. Wang, M. Yang, DNAzyme-Au nanoprobe coupled with graphene-oxide–loaded hybridization chain reaction signal amplification for fluorometric determination of alkaline phosphatase, Mikrochim. Acta 188 (2021) 7.
[26] J. Xue, L. Yang, Y. Jia, Y. Zhang, D. Wu, H. Ma, L. Hu, Q. Wei, H. Ju, Dual-quenching electrochemiluminescence resonance energy transfer system from Ru–In_2S_3 to α-MoO_3-Au based on protect of protein bioactivity for procalcitonin detection, Biosens. Bioelectron. 142 (2019), 111524.
[27] J. Xue, Q. Zhao, L. Yang, H. Ma, D. Wu, L. Liu, X. Ren, H. Ju, Q. Wei, Dual-mode sensing platform guided by intramolecular electrochemiluminescence of a ruthenium complex and cationic N,N-Bis(2-(trimethylammonium iodide) propylene) Perylene-3,4,9,10-tetracarboxydiimide for estradiol assay, Anal. Chem. 93 (2021) 6088–6093.
[28] S. Cheng, H. Liu, H. Zhang, G. Chu, Y. Guo, X. Sun, Ultrasensitive electrochemiluminescence aptasensor for kanamycin detection based on silver nanoparticle-catalyzed chemiluminescent reaction between luminol and hydrogen peroxide, Sens. Actuators B: Chem. 304 (2020), 127367.
[29] L. Yang, D. Fan, Y. Zhang, C. Ding, D. Wu, Q. Wei, H. Ju, Ferritin-based electrochemiluminescence nanosurface energy transfer system for procalcitonin detection using HWRGWVC heptapeptide for site-oriented antibody immobilization, Anal. Chem. 91 (2019) 7145–7152.
[30] J. Li, J. Jiang, D. Zhao, Z. Xu, M. Liu, P. Deng, X. Liu, C. Yang, D. Qian, H. Xie, Facile synthesis of Pd/N-doped reduced graphene oxide via a moderate wet-chemical route for non-enzymatic electrochemical detection of estradiol, J. Alloy. Compd. 769 (2018) 566–575.
[31] R. Wang, H. Chon, S. Lee, Z. Cheng, S.H. Hong, Y.H. Yoon, J. Choo, Highly sensitive detection of hormone estradiol E2 using surface-enhanced raman scattering based immunoassays for the clinical diagnosis of precocious puberty, ACS Appl. Mater. Interfaces 8 (2016) 10665–10672.
[32] C.-C. Chang, C.-Y. Yeh, Using simple-structured split aptamer for gold nanoparticle-based colorimetric detection of estradiol, Anal. Sci. 37 (2021) 479–484.
[33] S. Biswas, Y. Chen, Y. Xie, X. Sun, Y. Wang, Ultrasmall Au(0) inserted hollow PCN-222 MOF for the high-sensitive detection of estradiol, Anal. Chem. 92 (2020) 4566–4572.

Qinqin Zhao is a master student in school of chemistry and chemical engineering, University of Jinan. Her current researchers are electrochemiluminescence sensor and nanomaterials.

Jingwei Xue is a master student in school of chemistry and chemical engineering, University of Jinan. Her current researchers are electrochemiluminescence sensor and nanomaterials.

Xiang Ren received his B.S. degrees in Chemistry of Materials/English from University of Jinan in 2012, M.S. degree in Chemical Engineering and Technology from University of Jinan in 2015, and Ph.D. degree from University of Jinan/University of Electronic Science and Technology of China in 2019. Now, he is an associate professor in University of Jinan. His main research interests are energy catalysis, nanomaterials controlled-synthesis, and electrochemical biosensors.

Dawei Fan received her Ph.D. degree from Lanzhou institute of chemical physics, Chinese academy of sciences. Now, she is an associate professor at University of Jinan. Her main research interests are electrochemical sensors and photoelectrochemical sensors. She has published over 50 articles on analysis, immunosensor and applied successfully for many research projects, such as *Angewandte Chemie International Edition*, *Biosensors & Bioelectronics*, *Journal of Physical Chemistry C*, and *ACS Applied Materials & Interfaces*.

Xuan Kuang obtained her Ph.D. in Analytical Chemistry in 2015. Her research interests focus on metal organic materials and the application of nanomaterials to electrochemical sensors, synthesis and fundamental electrochemical studies of energy storage devices and synthetic nanomotors.

Yuyang Li received his Ph.D. degree from China University of Petroleum (East China) in 2018. His main research interest are the design and preparation of functional nanomaterial, sensor technology, fluorescence imaging, and their industrial application. He has been hosting one national scientific research project.

Qin Wei, a professor and DSc, has devoted herself to analytical teaching and scientific research. Her main research interests are the determination of protein and nucleic acid by photometry and the electrochemical immunosensor preparation. She has published over one hundred articles on analysis, immunosensor and applied successfully for many research projects, such as *Biomaterials, Adv. Funct. Mater., Biosens. Bioelectron., Sens. Actuators B: Chem., Talanta.*

Huangxian Ju received his B.S., M.S. and Ph.D. degrees from Nanjing University during 1982–1992. He was a postdoc in Montreal University (Canada) from 1996 to 1997 and a guest professor in three universities of Germany and Ireland in 1999–2000. He became an associate and full professor of Nanjing University in 1993 and 1999. He is currently the director of State Key Laboratory of Analytical Chemistry for Life Science. His research interests focus on analytical biochemistry, biosensing and molecular diagnosis. He has published 616 papers in different journals with SCI h-index of 83 (29,523 citations) and Google Scholar h-index of 91 with more than 29,000 citations.